Analysis of Bridge Performance Exposed to Earthquake and Flood Induced-Scour for Very Dense Sand: Derivation of Fragility Curves

Elwin Yu You Kuan[1], Nordila Ahmad[1,*], Siti Khadijah Che Osmi[1], Jestin Jelani[1], Zuliziana Suif[1], Edy Tonnizam Mohamad[2], Badronnisa Yusuf[3], Thamer Ahmed Mohammed[4]

1   Department of Civil Engineering, Faculty of Engineering, National Defence University of Malaysia, Sungai Besi Camp, Kuala Lumpur, Malaysia
2   Centre of Tropical Geoengineering (GEOTROPIK), Faculty of Civil Engineering, Universiti Teknologi Malaysia, Malaysia
3   Faculty of Engineering, Universiti Putra Malaysia, Malaysia
4   Department of Water Resources Engineering, College of Engineering, University of Baghdad, Iraq

ARTICLE INFO	ABSTRACT
Keywords: Fragility curves; earthquake; scour; seismic intensity; non-linear time history analysis; rc bridges; vulnerability assessment; median threshold	Bridges play a critical role in maintaining transportation networks, and their resilience to natural disasters is of utmost importance. The bridges' vulnerability to multiple hazards particularly seismic activities and flood-induced scour is not fully understand. This study focuses on evaluating how bridges respond to the simultaneous threats of earthquakes and flood-induced scour, particularly in very dense sandy soil conditions. The research employs specialized finite element modelling software (CSI Bridge) to derive fragility curves, providing crucial insights into bridge vulnerability in these challenging circumstances. This comprehensive approach allows for a thorough assessment of bridge vulnerability which primarily contribute to the development of fragility curves for minor, moderate and extensive damage. These curves quantify the probability of bridge damage or failure across varying levels of hazard intensity. Nonlinear time history analyses were conducted by 5 earthquakes data from the past events by scaling it within the range of 0.25 g to 1.5 g and various scour depth which ranges from no scour, $1D_f$, $1.5D_f$ and $2D_f$. The findings highlighted those bridges exposed to both earthquake and flood-induced scour in very dense sandy soils heightened the risks of damage and the median threshold value of the earthquake intensity measure (IM_{mi}) will show a lower value when the probability of damage is higher. Results demonstrate that the higher the depth of scour, the higher the probability for the bridge to undergo minor, moderate as well as extensive damage in very dense sandy soil type. Thus, it was concluded that the probable multi-hazard impacts of earthquake and scouring in river crossing bridges should be considered in bridge substructure design.

1. Introduction

The construction of bridges is a substantial undertaking that requires significant financial investment and careful attention to the crucial issue of bridge failure, mainly attributed to scouring. The erosion of piers is a vital aspect in the hydraulic design of bridges. Nonetheless, accurately assessing the wear and tear on the support pillars of the bridge in real-world conditions, especially

during intense rainfall, poses considerable challenges [1]. Bridges, as essential components of transportation networks, are critical to the uninterrupted flow of goods, services, and people in our modern societies [2]. Their functionality and resilience in the face of natural disasters are pivotal to maintaining the infrastructure's integrity and, by extension, the well-being of communities. The current approach to bridge engineering involves using separate hazard models for natural and manmade threats. Methods for estimating losses and mitigating risks in bridges are formulated by assessing their failure probabilities under specific hazard scenarios. Nevertheless, there is a possibility of consecutive occurrences of two extreme events within a relatively short timeframe [3]. The consequences of aging, heavier traffic loads, and natural disasters such as earthquakes, extreme rainfall, floods, and changing global climate are expected to exacerbate the challenges faced by bridges [4]. According to the study by Nasr *et al.,* [5], this could potentially impact the safety and future functionality of bridges. The limitations on river crossings can lead to significant disruptions in the network, especially when there are limited alternative routes, as multiple bridges within the same region along a river may collapse during intense storms. Heavy rainfall resulting in flooding can elevate river flows, leading to increased scouring around bridge foundations. The collapse of bridges and the consequential impact on various infrastructures, such as water reservoirs, hydropower plants, and sewage systems, have been documented in studies by Degefu and Bewket [6]. It has been suggested that increased flow exacerbates vortex scouring stresses on bridge supports, resulting in higher scour [7].

Scouring, defined as the removal of sediments like sand and rock from around bridge abutments or piers, is a phenomenon associated with high water flow in and around water bodies [8]. As the 2009 floods in Cumbria, UK, demonstrated, bridge infrastructure has been severely threatened by the issue of flooding. At least 20 bridges were destroyed or damaged as a result of this incident, which also had significant societal effects, one fatality, and repair expenses of £34 million [9]. Hydraulic considerations, especially flood and scour impacts, are frequently the main cause of reported bridge failures and may get worse due to climate change [10]. Apart from the challenges associated with flooding, large-scale seismic events have also presented a significant risk to bridges across the globe, mostly because of inadequate seismic design guidelines [11]. Yuan *et al.,* [12] showed that the Tohoku earthquake and tsunami in Japan in 2011 highlight how bridges are vulnerable to a variety of risks and domino effects, such as combinations of earthquake and flood, earthquake and aftershock, or earthquake-tsunami. The interdependence of these issues is demonstrated by the 2005 flooding catastrophe in Southern Italy that followed heavy rains and left six people dead and numerous more injured in addition to severely damaging roads, railroads, and other infrastructure [13]. Similar to this, the Canterbury earthquake sequence that struck New Zealand in 2010–2011 severely damaged road networks. This damage was ascribed to sand boils, water ponding on road surfaces, rock falls, liquefaction, settlements, and lateral spreading [14].

According to recent studies, 53% of bridge failures in the United States between 1989 and 2000 were caused by hydraulic factors including scouring and flooding. The country has its own unique set of problems. Furthermore, a contemporary issue that damages highway embankments is flooding in riverine and coastal areas [15]. According to Hamill [16], the local scour is produced when a normal flow encounters a pier and experiences an abrupt change in its normal flow pattern. The system of vortices or large-scale eddy structures forms at the base of the jetty. In typical eddy structures, two vortices are present. The vortices depicted in Figure 1 are the Horseshoe vortex and Wake vortex systems.
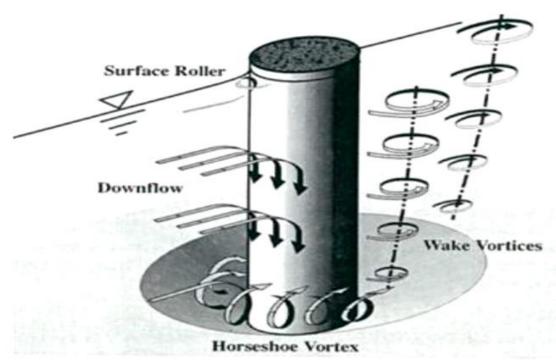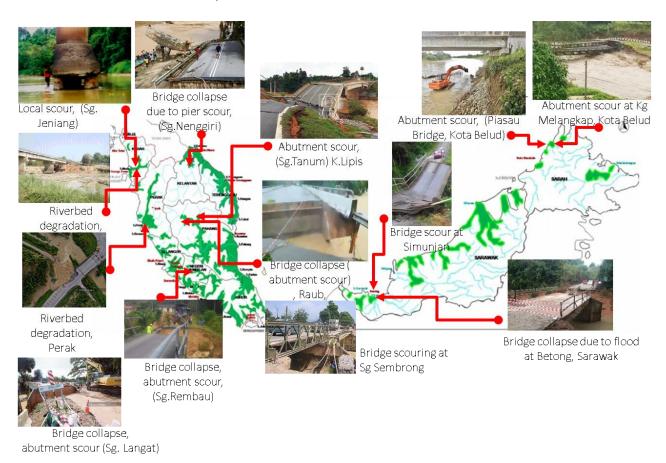
Fig. 1. Scour pattern at a circular pier (Hamill, 1998)

At a pier, a flow of a particular velocity ceases entirely, leading to an increase in water surface pressure in the vicinity of the pier. As the flow velocity decreases progressively from the top to the bottom, the pressure also decreases in a similar fashion. This generates a pressure differential that propels the flow in a downward direction akin to that of a water jet. This vertical discharge induces a fissure in the vicinity of the pier's base upon impacting the bed. The downward force is at its greatest magnitude immediately beneath the bed level. As the downward flow continues to generate an opening, it undergoes a transformation into a horseshoe-shaped vortex system when it interacts with the incoming flow; thus, the name horseshoe vortex. The horseshoe vortex is especially effective at particle removal from the jetty. Wake vortex formation results from pier flow separation. Sternal vortices erode pier sediment while in motion. Similar to a hoover, the wake vortex system is capable of attracting and transporting detritus. Due to the fact that the intensity of the wake vortices drastically decreases as one descends, sediment deposition frequently takes place directly downstream of the pier. Concurrently, horseshoe and wake vortices will scour the pier. Instability of the bridge is caused by erosion of the river bed, either through general or local scour around the piers. In Malaysia, the bridges that experiences scouring effect throughout the year of 2006 to 2021 were displayed in Figure 2. It shows that the scouring problem mostly occurred at piers and abutments.

Among the numerous challenges that bridges encounter, the combined hazards of earthquakes and floods stand out as formidable adversaries [17]. Earthquakes impose dynamic forces on bridges, while floods introduce scouring processes that can compromise their foundations. One of the most impactful natural disasters affecting global economies and populations is an earthquake, characterized by the abrupt movement along a fault line that induces ground shaking. This seismic energy is generated by the slip, volcanic activity, magmatic processes, or sudden stress changes in the Earth. The aftermath of an earthquake disaster includes surface rupture and the release of seismic waves, setting off a chain reaction of events such as tsunamis, landslides, liquefaction, and structural damage to buildings due to tremors [18]. There were a total of 2024 earthquakes that

occurred in Indonesia between January 2009 and August 2018, with magnitudes ranging from 5 to 8 on the Richter Scale, according to the data that was collected from the catalog of the United States Geological Survey in Indonesia, which is freely available to the public [19]. Given the wide range of potential disasters, such as earthquakes and floods, and the way in which these events can have cascading impacts, it is critical to undertake an impartial assessment of the risks and vulnerabilities that transport infrastructure faces. This method assures that resources are allocated effectively to the construction of robust transport networks.

Fig. 2. Location of bridge scour in Peninsular Malaysia and East Malaysia recorded from year 2006-2021 in flood-prone area

The importance of evaluating the vulnerability of bridges to natural disasters, specifically earthquakes and floods, owing to their substantial potential for inducing significant economic losses had been investigated by numerous scholars such as Argyroudis and Mitoulis [20], He *et al.,* [21], Yilmaz *et al.,* [22], Gehl and D'Ayala [23], Wang *et al.,* [24] and Dong *et al.,* [25]. These assessments typically involve the formulation of fragility curves. However, recent research endeavors have broadened their scope beyond the development of fragility curves tailored to individual hazards, instead directing their attention toward creating more intricate curves that account for the collective impact of climate change and various hazards on bridge infrastructure [26-28]. The combination of earthquake-induced ground motions and flood-induced scour in regions characterized by such soils can subject bridges to multifaceted and interconnected risks. The fragility assessments were performed to assess the seismic performance of the bridge in the presence of scouring effects. It was found that scouring has a significant unfavorable impact on the lateral response of the bridge [29]. Therefore, the present investigation offers an approach for assessing reinforced concrete (RC) bridges on how flood-induced scour affects bridges' seismic performance using nonlinear time

history analysis method. The analyses were executed using CSI Bridge v25.0.0. which is a finite element modelling (FEM) software. The objective of this study is to obtain the bridge response and the failure probability of the bridge under the combined effect of flood and earthquake in very dense sand.

2. Methodology
2.1 Numerical model of the bridge

The bridge under consideration is a fully integrated, three-span pre-stressed concrete structure with a length of 130 meters. Notably, this bridge design stands out for its absence of expansion joints or bearings. The structural configuration includes two outer spans, each measuring 40 meters, and one middle span measuring 50 meters. Complementing the design are abutments that extend to the full height of the structure. The deck, constructed as a box girder, boasts a total width of 13 meters. The abutments, towering at 18 meters in height, feature footings with a thickness of 1 meter and a length of 5.5 meters. Piers, exhibiting a circular profile with a diameter of 2.4 meters and a height of 20 meters, further contribute to the bridge's robust structure. The piers' footings, with a thickness of 1 meter and a length of 3.5 meters, fortify the overall stability of the bridge. The pile length is 14.5 m below the pile cap. This resilient structure is subjected to a distributed load of 18.5 kN/m/m, meticulously calculated to account for the combined weight of the deck and live loads as per Eurocode 8-Part1 standards. The C30/37 concrete, which has an elastic modulus (E) of 3.3×10^7 kN/m² and a unit weight (γ) of 25 kN/m³, was used as the carefully chosen construction material for the bridge components. 0.2 is the Poisson ratio that is used. Rebar with a unit weight of γ = 76.97 kN/m³ and an elastic modulus of E = 1.999×10^8 kN/m² makes up the reinforcement. The employed structural steel is of grade S355, with an elastic modulus of E=2.1×10^8 kN/m² and a unit weight of γ=76.97 kN/m³. The tendon of the bridge has an elastic modulus of E=1.965×10^8 kN/m² and a unit weight of γ=76.97 kN/m³. The bridge is supported by a pair of piers and two integral abutments that extend to their maximum height, as seen in Figure 3.
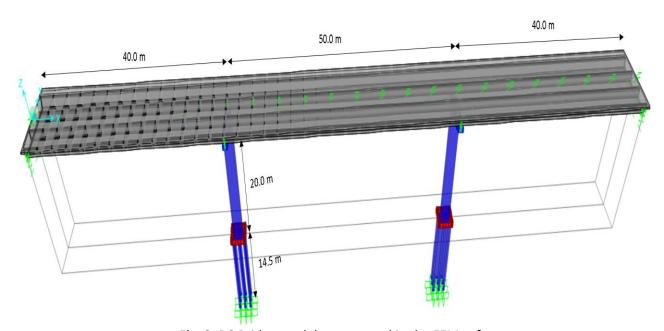

Fig. 3. RC Bridge model constructed in the FEM software

Figure 4 illustrated the required data for the concrete girder box section of the bridge which need to be inputted to the Finite Element Method (FEM). This data was necessary for the construction of the bridge section model. All the properties of the bridge and soil were inputted into the FEM using CSI Bridge software. The corresponding values can be found in Table 1.
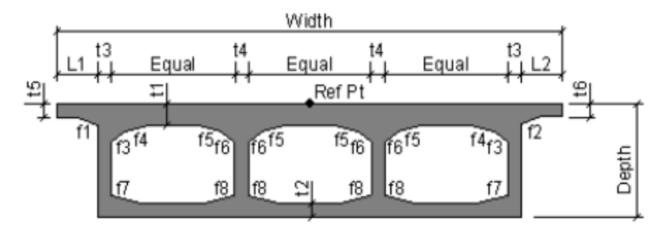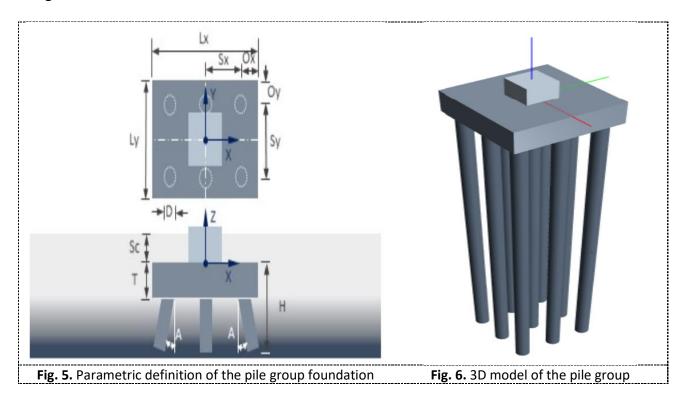

Fig. 4. Concrete box girder bridge section of the deck as required in FEM software

Table 1
Specifications for the concrete box girder's cross-sectional dimensions

General Data	Units
Material Property	C30/37
Number of Interior Girders	2
Total Width	13.00 m
Total Depth	2.1 m
Left Exterior Girder Bottom Offset (L3)	0.71
Right Exterior Girder Bottom Offset (L4)	0.71
Slab and Girder Thickness	Units
Top Slab Thickness (t1)	0.305 m
Bottom Slab Thickness (t2)	0.300 m
Exterior Girder Thickness (t3)	0.300 m
Interior Girder Thickness (t3)	0.305 m
Fillet Horizontal Dimension Data	Units
f1 Horizontal Dimension	0.10 m
f2 Horizontal Dimension	0.10 m
f3 – f8 Horizontal Dimension	0.00 m
Fillet Vertical Dimension Data	Units
f1 – f8 Vertical Dimension	0.15 m
Left Overhang Data	Units
Left Overhang Length (L1)	0.915 m
Left Overhang Outer Thickness (t5)	0.300 m
Right Overhang Data	Units
Right Overhang Length (L2)	0.915 m
Right Overhang Outer Thickness (t6)	0.300 m

The abutments are connected to the girder bottom only and supported with fixed foundation spring. The bridge foundation is supported by a group of pile and the relevant values used to model the pile group can be found in Table 2. There is only one soil type which is very dense sandy soil used in this study. Figure 5 showed the parameters that need to be specified in the CSI Bridge software in

order to facilitate the construction of the pile group model. The 3D model of the pile group is shown in Figure 6.

Fig. 5. Parametric definition of the pile group foundation **Fig. 6.** 3D model of the pile group

Table 2
Specifications for the pile group foundation

Pile Cap	Units
Footing Material	C30/37
Total Length, Lx (m)	3.50
Total Width, Ly (m)	3.50
Thickness, T (m)	1.00
Overhang, Ox (m)	0.45
Overhang, Oy (m)	0.45
Max Mesh Size (m)	1.00
Pile Group	**Units**
Pile Material	C30/37
Number of Piles – Nx	3
Number of Piles – Ny	3
Pile Diameter, D (m)	0.5
Pile Vertical Length, H (m)	15
Pile Spacing – Sx (m)	1.3
Pile Spacing – Sy (m)	1.3
Batter Angle Along X – Ax (deg)	0
Batter Angle Along X – Ay (deg)	0
Pile End Spring	Fixed translation along X, Y and Z and fixed rotation around X, Y and Z

In accordance with Eurocode 8-Part1 [30] specifications, the bridge experiences a distributed load of 20 kN/m/m, encompassing both live loads and the inherent self-weight of the deck. The definition of the bridge lane is established to pinpoint the areas on the superstructure where vehicle loads exert their influence. Specifically, three floating lanes are set at a width of 3.6576 meters. To model the p-

y curve for the foundation of the bridge, multilinear plastic link is chosen and the properties of the effective stiffness of very dense sandy soil based on ground type B, according to EN 1998-1 [30] is 152000 kN/m^2. For the dynamic analyses, five earthquake time histories were procured from the Pacific Earthquake Engineering Research Center (PEER) ground motion database, featuring seismic events such as Duzce (Duzce), Mw=7.14, Turkey, 1999; Kocaeli (Gebze), Mw=7.51, Turkey, 1999; Umbria Marche (Gubbio-Piana), Mw=5.7, Italy, 1997; Hector Mine (Hector), Mw=7.13, USA, 1999; and Fruli (Barcis), Mw=6.5, Italy, 1976. These earthquake data are employed in dynamic analyses with their time histories scaled to increase Peak Ground Acceleration (PGA) from 0.25 g to 1.50 g at intervals of 0.125 g. Nonlinear modal time history analyses for various load cases have been introduced, utilizing earthquake data scaled down to PGAs ranging from 0.25 to 1.50 g. A constant damping of 5% is applied across all modes. The scale factor for each earthquake event is calculated using Eq. (1) [31] and is incorporated into the CSI Bridge for nonlinear dynamic time history analyses. The bridge model undergoes scrutiny under varying scour depths to assess structural damage, with a foundation depth (D_f) set at 1.2 meters. The study encompasses scouring based on the foundation depth, ranging from no scour to $1D_f$, $1.5D_f$, and $2D_f$. Consequently, a comprehensive analysis is conducted, considering a total of 220 combinations for the bridge model. These combinations involve one distinct type of soil, specifically very dense sandy soil, five seismic inputs, eleven levels of PGA, and four scour depths.

$$Scale\ Factor, f = \frac{Anticipated\ PGA}{Real\ PGA} \tag{1}$$

2.2 Construction of the seismic fragility curves based on variable scour depth

The PGA under bedrock settings is the earthquake intensity measure (IM) used to establish the fragility function, which is a mathematical model that quantifies the probability of surpassing particular limit states. As demonstrated in Eq. (2) [32-33], a lognormal probability distribution function is a typical characterization of fragility curves. Two parameters, IM_{mi} (the median threshold value of IM needed to cause the ith damage state) and β_{tot} (the overall lognormal standard deviation), are set up during the design phase.

$$P(DS \geq DSi|IM) = \Phi\left[\frac{In\left(\frac{IM}{IM_{mi}}\right)}{\beta_{tot}}\right] \tag{2}$$

Fragility functions for the pier component of the bridge were generated using the correlation between the intensity measure (IM), specifically the peak ground acceleration (PGA) for earthquakes, and the engineering demand parameters (EDP). The maximum vertical displacement of the pier is determined through taking into account different seismic hazard actions and accounting for the uncertainty in the demand (B_D) based on very dense sandy soil. The determination of the overall variability (β_{tot}) takes into account three factors of uncertainty and is carried out following Eq. (3), assuming statistical independence. According to Yuan *et al.,* [12], the uncertainty related to the definition of damage states (β_{ds}) is predetermined to be 0.4, whereas the uncertainty related to capacity (β_C) is established at 0.3 based on judgement by experts. The standard deviation of the residuals between the computed EDP and the best fit regression is used to evaluate the extent of uncertainty in response to hazard actions (B_D).

$$\beta_{tot}^2 = \beta_C^2 + \beta_D^2 + \beta_{ds}^2 \tag{3}$$

The drift ratios are considered as a substitute EDP for the pier, and the damage index thresholds were according to Jain *et al.,* [34] as detailed in Table 4.

3. Results
3.1 Development of fragility curves for pier

Three scour depths were applied to the constructed models, beginning with the initial state having no scour, followed by three scour depths of $1D_f$, $1.5D_f$, and $2D_f$. Following that, the constructed models undergo a non-linear dynamic analysis in which each model is exposed to a variety of Peak Ground Accelerations (PGA) ranging from 0.25 g to 1.5 g. As illustrated in Figure 7, the relationship between the applied ground motions and the drift percentage for the selected pier with joint number 168 of the bridge model is established by calculating the maximum drift percentage from the pier's maximum displacement. Jain *et al.,* [34] conducted the calculation of the damage index for the structures through the application of drift percentage limitations. The progression of damage for pier drift ratio at varied scour depths and PGA was plotted. In order to derive the natural logarithm of the IM_{mi}, it must ascertain the intersection point of the best-fit line. Damage evolution with the IM of an earthquake is demonstrated in the paper by Argyroudis and Kaynia [35]. This includes the calculation of the IM_{mi} for a particular damage state (d_{si}) and the standard deviation (β_D), which is affected by the variability in input motion.
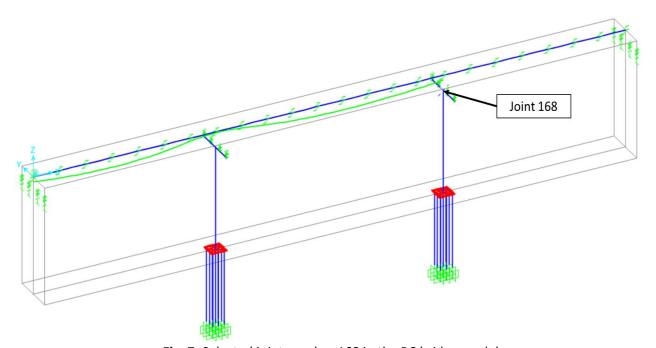

Fig. 7. Selected joint number 168 in the RC bridge model

For the purpose of calculating the β_{tot} based on Eq. (3), it is necessary to have the β_D value, which may be obtained by utilizing the coefficient of determination r^2 of the line that provides the best fit in the regression curves. The β_{tot} and β_D values of every single bridge model that has been developed are distinct from one another due to the fact that they are influenced by the maximum displacement of the joint 168, which is influenced by the different scour depths constructed models. When the scour depth changes, it will have an effect on the calculation of the drift ratio, which will result in a

range of results as the regression curves vary. A summary of the values of β_{tot} and β_D may be found in Table 3 while Tables 4 shows the value for IM_{mi}. These results were obtained when the model was subjected to varying degrees of scour depth, including no scour, $1D_f$, $1.5D_f$, and $2D_f$.

Table 3
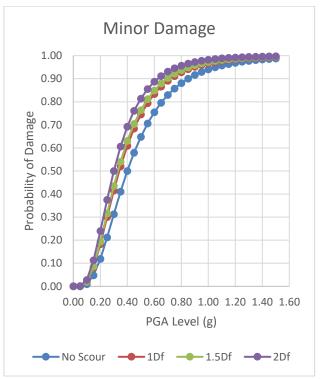Determining the β_D and β_{tot} based on various scour depths

Scour Depth	β_D	β_{tot}
0	0.32	0.59
$1D_f$	0.31	0.59
$1.5D_f$	0.29	0.58
$2D_f$	0.28	0.57

Table 4
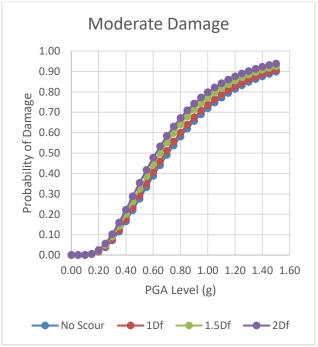Determining the IM_{mi} for highly dense sandy soil under various scour depth condition in the regression curves

				Scour Depth			
				No Scour	$1D_f$	$1.5D_f$	$2D_f$
Damage States	Drift (%) Limits	Damage Index (DI)	Ln DI	IM_{mi} (g)			
Minor	0.7	0.13	-2.04	0.40	0.34	0.33	0.30
Moderate	1.5	0.27	-1.31	0.71	0.69	0.65	0.62
Extensive	2.5	0.45	-0.80	1.27	1.24	1.22	1.11

For the bridge model, fragility studies are carried out at every possible combination of scour depths and earthquake intensities. It is possible to establish the fragility curves at the minor, moderate, and extensive states separately. The fragility curves of Pier 2 with joint 168 are displayed in Figure 8, 9 and 10. This joint is subject to different scour depths of 0, 1Df, 1.5Df, and 2Df followed by various seismic PGA levels from 0.25 g to 1.5 g. The curves in Figure 8 showed all the scour depth based on minor damage state whereas in Figure 9 and 10 displayed the values for the various scour depth from 0 to 2Df to identify the changes based on moderate and extensive damage states. Therefore, the evaluation of bridge performance, specifically focusing on the seismic response of piers and piles under the combined impact of scour and earthquake, can be conducted through nonlinear time history analysis.
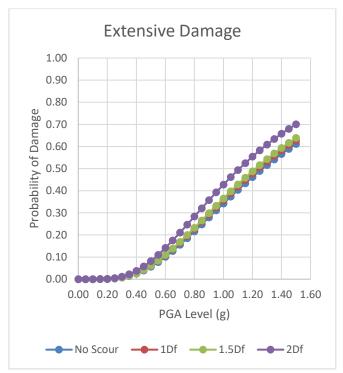
The IMmi values provide a relative measure of the impact on various scour depths on the performance of bridge model under seismic loading. Seismic fragility characteristics of bridge models are compared in terms of the IMmi obtained for various combinations of scour depth and PGA levels. With increase in IMmi, the probability of damage under minor, moderate, and extensive damage decreases. Figure 8 showed that the curves for 2Df have the highest probability of damage while no scour curve showed the lowest probability of damage in the minor damage. At a PGA of 0.70 g, the probability of damage under 2Df condition is 93.05% follow by 90.31% under 1.5Df, 89.10% for 1Df and lastly 82.93% for no scour condition. The fragility curves at moderate damage presented that the probability of damage from the highest to the lowest as it showed a similar trend through different combination of seismic intensities and scour depths. Figure 9 shows that as the PGA increases, the probability of damages also increase which correlates that higher scour depth will have more chances of damages. This can be seen that the probability of damage to reach 50%, the scour depth of 2Df showed a value of 53.29% at 0.65 g whereas it only reaches 50.00% at the same PGA level of 0.65 g in 1.5Df scour depth. In addition, the 1Df scour depth only reaches 50.98% at 0.7 g and 49.04% in no scour condition at the same PGA level. Next, fragility curves for extensive damage states were observed in Figure 10, the 2Df showed the highest probability of damage where it reaches 70.05% at 1.5 g while other scour depths only reach 63.87%, 62.73% and 61.14% for 1.5Df, 1Df and no scour respectively. It can be shown that the vulnerability of the bridge varies greatly depending on the

scour conditions and seismic loads. Overall, the results reveal that the scour hazard, particularly for more severe occurrences such as scour depths of 2Df, constituted a major threat to bridge sections at all damage levels. This is a reasonable result for an integral bridge with a deep foundation.

Fig. 8. Fragility curves of RC bridge pier model undergoes various scour depth and seismic effect of different PGA levels at minor damage states

Fig. 9. Fragility curves of RC bridge pier model undergoes various scour depth and seismic effect of different PGA levels at moderate damage states

Fig. 10. Fragility curves of RC bridge pier model undergoes various scour depth and seismic effect of different PGA levels at extensive damage states

4. Conclusions

This paper introduces a methodology that combines distinct models for seismic and flood hazards to study the vulnerability of bridges to seismic events when affected by flood-induced scour. The fragility curves are used to quantify the damageability of RC bridges in the context of flood-induced scour during an earthquake in a multi-hazard scenario. The results suggest that the pier's ability to withstand seismic occurrences decreases when the value of IMmi is smaller, as it becomes a greater probability to sustain minor, moderate, and extensive damage. The evaluation has indicated the probability of multiple levels of damage for a pier, taking into account a range of PGA up to 1.50 g and varying depths of scour up to twice the foundation depth (2Df). Furthermore, it has been demonstrated that there is a correlation between the likelihood of structural damage and the increase in both seismic intensity and scour depth. The impact of scour depths on the seismic performance of the bridge was more significant in the 2Df scenario compared to other scour depths, such as 1.5Df, 1Df, and during the absence of scour. The probability of damage significantly increases as the scour depth increases and this can also be anticipated when the IMmi value become smaller as the removal of soil causes the instability of the exposed pile group. Furthermore, the length of bridge piers has an impact on their fragility characteristics. Bridges that include longer bridge piers exhibit higher IMmi values, which indicate a reduced vulnerability to seismic risks. Moreover, the seismic performance of bridges might differ based on factors such as the kind of bridge, subsurface conditions, and the features of natural disasters like floods and earthquakes. Future research could investigate the impact of scour depth and seismic intensity on various components of bridges, including bridge bearings, diaphragm abutments, expansion joints, and stratified soil with different properties. Additionally, the study could expand its analysis to include other potential factors that could lead to failure, such as corrosion and tsunami.

Acknowledgement

References

[1] Noor, Muqadas, Humaira Arshad, Mujahid Khan, Mahmood Alam Khan, Muhammad Sagheer Aslam, and Afnan Ahmad. "Experimental and HEC-RAS modelling of bridge pier scouring." *Journal of Advanced Research in Fluid Mechanics and Thermal Sciences* 74, no. 1 (2020): 119-132. https://doi.org/10.37934/arfmts.74.1.119132

[2] Smith, J. R., & Brown, A. L. (2020). Earthquake-induced scour in sandy soils: A comprehensive review. *Geotechnical Engineering Journal*, 45(2), 112-128.

[3] Ganesh Prasad, G., & Banerjee, S. (2013). The impact of flood-induced scour on seismic fragility characteristics of bridges. *Journal of Earthquake Engineering*, 17(6), 803-828. https://doi.org/10.1080/13632469.2013.771593

[4] Dikanski, Hristo, Boulent Imam, and Alex Hagen-Zanker. "Effects of uncertain asset stock data on the assessment of climate change risks: A case study of bridge scour in the UK." Structural Safety 71 (2018): 1-12. https://doi.org/10.1016/j.strusafe.2017.10.008

[5] Nasr, Amro, Ivar Björnsson, Daniel Honfi, Oskar Larsson Ivanov, Jonas Johansson, and Erik Kjellström. "A review of the potential impacts of climate change on the safety and performance of bridges." *Sustainable and Resilient Infrastructure* 6, no. 3-4 (2021): 192-212. https://doi.org/10.1080/23789689.2019.1593003

[6] Degefu, Mekonnen Adnew, and Woldeamlak Bewket. "Variability and trends in rainfall amount and extreme event indices in the Omo-Ghibe River Basin, Ethiopia." Regional environmental change 14 (2014): 799-810. https://doi.org/10.1007/s10113-013-0538-z

[7] Barkdoll, Brian D. "Effects of climate change on bridge scour." In World Environmental and Water Resources Congress 2012: Crossing Boundaries, pp. 2532-2537. 2012. https://doi.org/10.1061/9780784412312.253

[8] Pizarro, Alonso, Salvatore Manfreda, and Enrico Tubaldi. "The science behind scour at bridge foundations: A review." Water 12, no. 2 (2020): 374. https://doi.org/10.3390/w12020374

[9] Cumbria Intelligence Observatory. "Cumbria floods November 2009: An impact assessment." (2010).

[10] Wardhana, Kumalasari, and Fabian C. Hadipriono. "Analysis of recent bridge failures in the United States." Journal of performance of constructed facilities 17, no. 3 (2003): 144-150. https://doi.org/10.1061/(ASCE)0887-3828(2003)17:3(144)

[11] Moehle, J. P., and M. O. Eberhard. "EARTHQUAKE DAMAGE TO BRIDGES. IN: BRIDGE ENGINEERING: SEISMIC DESIGN." (2003). https://doi.org/10.1201/9781420039788.ch2

[12] Yuan, Leung Fo Vincent, Sotirios A. Argyroudis, Enrico Tubaldi, Maria Pregnolato, and Stergios A. Mitoulis. "Fragility of bridges exposed to multiple hazards and impact on transport network resilience." In Proceedings of the 2019 Society for Earthquake and Civil Engineering Dynamics conference (SECED 2019). Society for Earthquake and Civil Engineering Dynamics (SECED), 2019.

[13] Polemio, M., and P. Lollino. "Failure of infrastructure embankments induced by flooding and seepage: a neglected source of hazard." Natural Hazards and Earth System Sciences 11, no. 12 (2011): 3383-3396. https://doi.org/10.5194/nhess-11-3383-2011

[14] Kongar, Indranil, Simona Esposito, and Sonia Giovinazzi. "Post-earthquake assessment and management for infrastructure systems: learning from the Canterbury (New Zealand) and L'Aquila (Italy) earthquakes." Bulletin of earthquake engineering 15 (2017): 589-620. https://doi.org/10.1007/s10518-015-9761-y

[15] Briaud, J. L., & Maddah, L. (2016). Minimizing roadway embankment damage from flooding (No. Project 20-05 (Topic 46-16)).

[16] Hamill, Les. Bridge hydraulics. CRC Press, 1998. https://doi.org/10.1201/9781482271638

[17] Kim, Hyunjun, Sung-Han Sim, Jaebeom Lee, Young-Joo Lee, and Jin-Man Kim. "Flood fragility analysis for bridges with multiple failure modes." *Advances in Mechanical Engineering* 9, no. 3 (2017): 1687814017696415. https://doi.org/10.1177/1687814017696415

[18] Noh, Muhammad Ramzanee Mohd, Shuib Rambat, Ida Sharmiza Binti Abd Halim, and Fauzan Ahmad. "Seismic Risk Assessment in Malaysia: A Review." *Journal of Advanced Research in Applied Sciences and Engineering Technology* 25, no. 1 (2021): 69-79. https://doi.org/10.37934/araset.25.1.6979

[19] Lenggana, Bhre Wangsa, Ubaidillah Ubaidillah, Fitrian Imaduddin, Widyarso Widyarso, Endra Dwi Purnomo, Dewi Utami, and Saiful Amri Mazlan. "Performance prediction of a novel modular magnetorheological damper for seismic building." *Journal of Advanced Research in Fluid Mechanics and Thermal Sciences* 58, no. 2 (2019): 275-286.

[20] Argyroudis, Sotirios A., and Stergios Aristoteles Mitoulis. "Vulnerability of bridges to individual and multiple hazards-floods and earthquakes." Reliability engineering & system safety 210 (2021): 107564. https://doi.org/10.1016/j.ress.2021.107564

[21] He, Haifeng, Kai Wei, Jiarui Zhang, and Shunquan Qin. "Application of endurance time method to seismic fragility evaluation of highway bridges considering scour effect." *Soil Dynamics and Earthquake Engineering* 136 (2020): 106243. https://doi.org/10.1016/j.soildyn.2020.106243

[22] Yilmaz, Taner, Swagata Banerjee, and Peggy A. Johnson. "Performance of two real-life California bridges under regional natural hazards." *Journal of Bridge Engineering* 21, no. 3 (2016): 04015063. https://doi.org/10.1061/(ASCE)BE.1943-5592.0000827

[23] Gehl, P., and D. D'Ayala. "Integrated Multi-Hazard Framework for the Fragility Analysis of Roadway Bridges. 12th Int." In Conf. Appl. Stat. Probab. Civ. Eng, pp. 12-15.

[24] Wang, Zhenghua, Jamie E. Padgett, and Leonardo Dueñas-Osorio. "Risk-consistent calibration of load factors for the design of reinforced concrete bridges under the combined effects of earthquake and scour hazards." Engineering Structures 79 (2014): 86-95. https://doi.org/10.1016/j.engstruct.2014.07.005

[25] Dong, You, Dan M. Frangopol, and Duygu Saydam. "Time-variant sustainability assessment of seismically vulnerable bridges subjected to multiple hazards." Earthquake Engineering & Structural Dynamics 42, no. 10 (2013): 1451-1467. https://doi.org/10.1002/eqe.2281

[26] Stefanidou, Sotiria P., and Andreas J. Kappos. "Methodology for the development of bridge-specific fragility curves." Earthquake Engineering & Structural Dynamics 46, no. 1 (2017): 73-93. https://doi.org/10.1002/eqe.2774

[27] Tsionis, G., and M. N. Fardis. "Seismic fragility of concrete bridges with deck monolithically connected to the piers or supported on elastomeric bearings." In 15th world conference of earthquake engineering. 2012.

[28] Nielson, Bryant G., and Reginald DesRoches. "Seismic fragility methodology for highway bridges using a component level approach." Earthquake engineering & structural dynamics 36, no. 6 (2007): 823-839. https://doi.org/10.1002/eqe.655

[29] Guo, Xuan, Yingkui Wu, and Ya Guo. "Time-dependent seismic fragility analysis of bridge systems under scour hazard and earthquake loads." Engineering Structures 121 (2016): 52-60. https://doi.org/10.1016/j.engstruct.2016.04.038

[30] Code, Price. "Eurocode 8: Design of structures for earthquake resistance-part 1: general rules, seismic actions and rules for buildings." Brussels: European Committee for Standardization (2005).

[31] Haselton, C. B., A. S. Whittaker, Ayse Hortacsu, J. W. Baker, Jonathan Bray, and D. N. Grant. "Selecting and scaling earthquake ground motions for performing response-history analyses." In Proceedings of the 15th world conference on earthquake engineering, pp. 4207-4217. Oakland, CA, USA: Earthquake Engineering Research Institute, 2012.

[32] Argyroudis, Sotirios, Stergios Mitoulis, Mike G. Winter, and Amir M. Kaynia. "Fragility of critical transportation infrastructure systems subjected to geo-hazards." In Proceedings 16th European Conference on Earthquake Engineering. European Conference on Earthquake Engineering, 2018. https://doi.org/10.1061/9780784481479.018

[33] Mackie, K. R., and B. Stojadinović. "Performance-based seismic bridge design for damage and loss limit states." Earthquake engineering & structural dynamics 36, no. 13 (2007): 1953-1971. https://doi.org/10.1002/eqe.699

[34] Jain, Ankit, Robin Davis, and CG Nanda Kumar. "Seismic fragility analysis of bridge pier." In IOP Conference Series: Materials Science and Engineering, vol. 936, no. 1, p. 012014. IOP Publishing, 2020. https://doi.org/10.1088/1757-899X/936/1/012014

[35] Argyroudis, Sotiris, and Amir M. Kaynia. "Analytical seismic fragility functions for highway and railway embankments and cuts." Earthquake Engineering & Structural Dynamics 44, no. 11 (2015): 1863-1879. https://doi.org/10.1002/eqe.2563